Experimental Validation of Pressure Distribution Prediction under Delta Wing Apex Vortex at High Reynolds Numbers

Open Access

Iddir Boumrar[1,*] and Ridha Djebali[2]

[1] Department of Mechanical Engineering, University Mouloud Mammeri of Tizi-Ouzou, Algeria
[2] Laboratory of Subatomic Physics, Nanosciences and Energetics, IPEST, University of Carthage, Tunisia

ARTICLE INFO	ABSTRACT
	This study presents an application of the Fluent CFD methodology to solve Navier-Stokes equations, for the forecast of flow implying evolution of principal vortices developed on suction face of a thin delta wing. A delta wing model with apex angle β=80° is subjected to measurements in subsonic wind tunnel and defect pressure coefficient values reached under the apex vortex core are obtained via a row of pressure taps. Numerical simulations are carried out for the same experimental delta wing model at angle of attack *i*=15°, before the vortex bursting, and at Reynolds number based on the wing chord Re=1.0840×10⁵. Numerical predictions of defect pressure coefficient −Cp are compared to experimental data. Good agreement is obtained between predictions and measurements. Pressure and velocity evolutions at different cross-sections of the longitudinal vortex were also considered allowed us to reveal clearly the apex vortex core. The numerical results analysis in several cross sections reveals a peak distinct under the principal apex vortex. At the studied delta wing suction face the defect pressure coefficient reaches maximal value close to 2.5 which agrees with that found in literature.

1. Introduction

The apex vortex is a very dominant phenomenon in flow over delta wings used generally on modern aircraft fighters. While the vortices present advantages to increase the lift via high fields of suction above the delta wing, a phenomenon called vortex bursting can lead to serious problems of instabilities during flight.

Corresponding author.
E-mail address: boumrari@hotmail.fr (Iddir Boumrar)

In practical, the apex vortices intensity increases with the wing angle of attack; the beginning of the vortex bursting, however, determines the maximum of induced vortex lift which can be reached during such operations. Vortex bursting deteriorates also the apex vortex additional lift.

Advantages implied by the apex vortex at high angles of attack for various modes of flow justified many following experimental, theoretical and numerical investigations. Scott Morton *et al.,* [1] demonstrate the ability of Detached-Eddy Simulation, and hybrid RANS-LES model, to predict the vortex breakdown at Reynolds numbers above 10^6.

Experiments performed at ONERA using LDV and pressure measurement were used to compare numerical simulations results what utilizing both RANS and DES turbulence models. The flow field equations past a 70° sharp edged delta wing in a subsonic free stream were resolved by Anand Kumar [2] using the embedded conical grid. The breakdown is found to begin as a rapid deceleration of the core due to sudden increase in adverse axial pressure gradient. The presented results are expected to understand vortex breakdown in other flow situations.

Bandyopadhyay [3] studied the flow over a flat plate delta wing at incidence and in sideslip using vortex lattice models based on stream wise paneling. The theoretical values are compared to available theoretical and experimental results.

Delta wings with sweep angles of 45°, 50° and 55° were studied numerically by Hredesh and Tide [4] using RANS calculations coupled with SST k-ω turbulence model. Five different wing configurations were considered: sharp edged, semicircular, round, semi chamfered and double chamfered leading edges. Surface oil flow visualization measurements reported by Verhaegen (2011) were used for validation. The numerical studies on leading edge shapes show that round leading edge gives better values of lift as compared to other leading edge shapes tested. Size, location and strength of the vortex and breakdown location of the vortex core were affected considerably by the geometrical parameters.

Anwar-ul-Haque *et al.,* [5] presented a fully structured grid on a half span delta wing. Grids were refined near the wall to capture the physics of vortex flow in both the span and stream wise directions. The flow separation has been under-predicted by SA, Standard k-ε and RNG k-ε turbulence models. On the basis of comparison of computed surface pressure plots with that of experimental data and visualization of different contours, Shear Stress Transport model (SST) is found to be a good choice for prediction of separated flow over delta wing configurations. The primary vortex suction peak is situated conically on the wing and diminishes by moving toward the trailing edge. Surface flow visualizations show a sensitivity of the vortex structures to the angle of attack.

Bao-Feng Ma *et al.,* [6] Investigated the symmetry breaking and naturally occurring instabilities over thin slender delta wings with sharp leading edges. The study was carried out in a water tunnel using particle image velocimetry (PIV) measurements. Three delta wings models with 75°, 80° and 85° sweep angles over a range of angles of attack were considered. Properties of the vortex pairs depend only on the similarity parameter, which is a function of the angle of attack and the sweep angle. It was shown that vortex pairs develop asymmetry gradually with increasing the similarity parameter. Vortex asymmetry can develop in the absence of vortex breakdown on the wing. The vortex modes reveal the fluctuations of vorticity magnitude and helical displacement of the cores with little periodicity. There is little correlation of the fluctuations in the cores of the vortices.

Verhaagen [7] tested experimentally three 50° swept delta wing models. The first has a sharp leading edge and two others have a semi-circular leading edge of different radius. The vortical flow developed at the models faces was investigated using oil-flow visualization and Stereo Particle Image Velocimetry (SPIV) technique. It has been deduced that the leading-edge radius affects the size and strength of the vortices and the vortex core breakdown location over the models. The

results show that forces and moment acting on the delta wing are also affected. The flow structure over such wing depends on Reynolds number.

James Brett, Andrew Ool [8] used CFD simulations to analyze the vortical flows over sharp edged delta wings with sweep angles from 43° to 65° under subsonic conditions at angle of attack 10°. The flow field was assessed by comparing simulated results with experimental data. The shadow vortex was observed for sweep angles of 50° and less, and resulted in reduced lift production near the wing tips.

Nurulhuda Tajuddin *et al.,* [9] investigated the flow characteristics developed on the upper surface of the VFE- 2 blunt edged delta wing profiles at high angle of attack; this flow physics is very complicated. The vortex on the blunt-edged wing is developed at a certain cord wise position based on angle of attack, Reynolds number and leading edge bluntness. Measurement of pressure distribution were performed at Re=1×10^6 and 2×10^6, and tuft method was also performed to visualize the flow characteristics above the delta wing surface at high angle of attack. Result of both methods show that the primary vortex moves upstream close to the apex at high angles of attack.

Nadhirah Mohd Zain *et al.,* [10] conducted an experiment study of active flow control applied on the sharp-edged generic delta wing UAV at a speed of 18 m/s, the experiments were performed in a Low Speed wind tunnel sized of 1.5 x 2.0 meter^2. This work focuses on the effect of rotating propeller on the vortex properties above a generic 55^0 swept angle model with an overall length of 0.99 meter. Three configurations were tested: model without propeller followed by model with propeller diameter of 13" and diameter of 14". The results obtained indicate that the lift is increased particularly at high angle of attack. The results also show that vortex breakdown is delayed further aft of the wing when propeller rotating at about 5000 RPM.

Nelson and Visser [11] used experimental x-wire measurements of the flow field above a 70 ° and 75° flat plate delta wing at a Reynolds number of 2.5×10^5 and angles of attack of 20° and 30°. The spanwise distribution of axial vorticity is altered through the breakdown region and the amount of vorticity appears to reach a maximum immediately preceding breakdown. The axial vorticity components with an opposite direction, such as that found in the secondary vortex, seem to remain unaffected by changes in wing sweep and angle of attack.

A review of experimental results focused on pressure distributions was presented by Luckring [12]. The results demonstrate significant effects of leading-edge vortex separation. The objective was to distinguish the effects of Reynolds number, Mach number, angle of attack and leading edge bluntness on separation-induced leading-edge vortex flow common to slender wings.

Lok Sun Ko and Tim Lee [13] conducted a dye flow visualization around a slender delta wing with a sweeping angle of 65° with apex and tail flap control at a Reynolds number Re = 12900. The investigation revealed vortex breakdown (VBD) location over the different wing configurations. The flow visualization showed that a tail flap with anhedral deflection angle of -15° or -30° promoted VBD while a tail flap with dihedral deflection angle of +15° or +30° delayed VBD. A combination of apex flap -15° and tail +30° delayed VBD.

Lee and Ko [14] investigated a 65° sweep delta wing experimentally by apex flap and tip flap, deflected both independently and jointly. The drooped apex flap produced a higher lift at medium-to-high angle of attack and a delayed stall. The anhedral, introduced by the downward tip flap, generally promoted lift increment, whereas dihedral had the opposite effect. The joint apex and tip flap deflection gave a delayed leading edge vortex breakdown and an enhanced lift. The bursting behavior was not affected.

Guangxing Wu [15] used particle image velocimetry and pressure measurement techniques to study asymmetric vortex breakdown flow over three delta wings with sweep angle of 70°, 80°and 85°. The experiments were carried out in a wind tunnel at high angles of attack and Reynolds

number of 1.215×10^6. First, vortex breakdown flow over the 70° swept wing was found to be symmetric, whereas flow is asymmetric over the 80° and 85° swept wings. Instability due to crowding together of both leading-edge vortices is the cause of asymmetric vortex breakdown flow. Unpredictable manufacturing imperfection at the nose tip was found to lead uncertain asymmetric vortex breakdown flow.

Computational Fluid Dynamics methods are strongly implied in such extreme states of flow, and facilitate the evaluation of the starting criteria in terms of stability and ordering covering the unstable modes of flow as shown in work of Zhu and Jia [16]. A complete evaluation of stability properties can be obtained by the complete simulation of a plane by CFD methods coupled to mechanics of flight methods. Several works based on CFD simulation were conducted to calculate the turbulent flow and to test the vortex bursting on thin delta wings in comparison to previous experimental data by the authors [17]. The precise simulation of the experimental turbulent flows and the vortex bursting are significant. This is because captured characteristics of the bursting determine the distribution of pressure above the wing surface.

The present work is a methodological application of CFD with a choice for the meshing method made under available data-processing sources. This simulation provides the results which can be contrasted with those obtained experimentally by testing a model in a wind tunnel, simultaneously undertaken in order to test the validity of the CFD results.

2. Methodology

The experimental device is composed of a subsonic wind tunnel having a vein of 100 cm length with a test section 30x30 cm^2, with adjustable speeds from 0 to 45 m/s. It is supplemented by 24 multi-manometer tubes allowing measurements of pressure by reading the heights of oil prevailing in the tubes. The velocity measurement of air flow in the wind tunnel test section is ensured by a double pitot probe connected to a multi-manometer and by the Bernoulli formula as:

$$V_o = \sqrt{\frac{2\rho_H g \Delta h}{\rho}}$$ (1)

Besides, a suitable supports allow fixing of the wing in the test vein and connection of the pressure taps to the multi-manometer [18].

2.1. Wing Model

The subsonic flow around thin delta wing, with apex angle β= 80°, was considered in the present experimental study, the delta wing has a plane surface S=76.4cm^2, the wing chord is 955 millimeters. The Reynolds number Re based on the wing chord is close to 1.0840×10^5.

The smoke visualizations carried out by Leray *et al.,* (1985) [19] showed that it is possible to determine the angles value α_1 between the apex vortices, as well as the vortex structure symmetry developing on the delta wing suction face on both sides of its center line (Figure 1). For such reason, we laid out the pressure taps only on the right half of the wing.
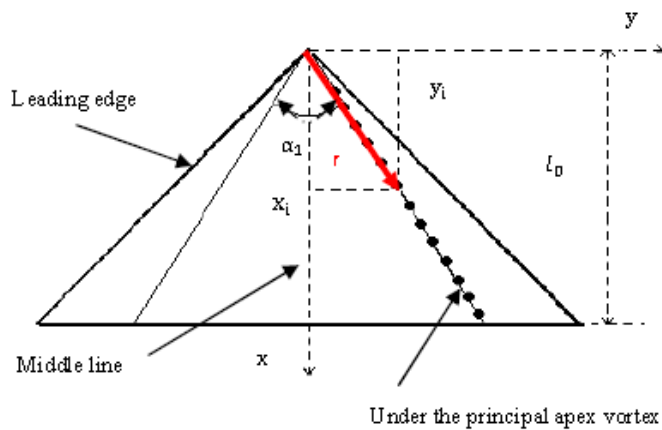
Fig. 1. Pressure taps positions under apex vortex of a delta wing model. Right: Model schematic view and left: realized model

2.2. Experimental Procedure

To follow the defect pressure prevailing under the apex vortex developed over a thin delta wing suction face (at the position $\alpha_1/2$) a pressure taps row is located under the vortex, then series of tests were undertaken and the defect pressure coefficient is obtained from measurements using the following relation:

$$p - p_0 = \rho_H g \, \Delta h \tag{2}$$

The coefficient Cp is then deduced as:

$$C_p = \frac{p - p_0}{\frac{1}{2}\rho V_0^2} = \frac{\rho_H g \, \Delta h}{\frac{1}{2}\rho V_0^2} \tag{3}$$

Figure 2 depicts the curves relating defect pressure coefficient evolution, under the delta wing apex vortex, according to various incidences $i(°)$. The coefficient –Cp increases with the incidence i until a critical incidence (i_{cr}=22°), corresponding to the vortex breakdown, where a clear change in "–Cp" evolution occurred. The plot corresponding to the critical incidence i_{cr}=22° falls down relatively to the others.

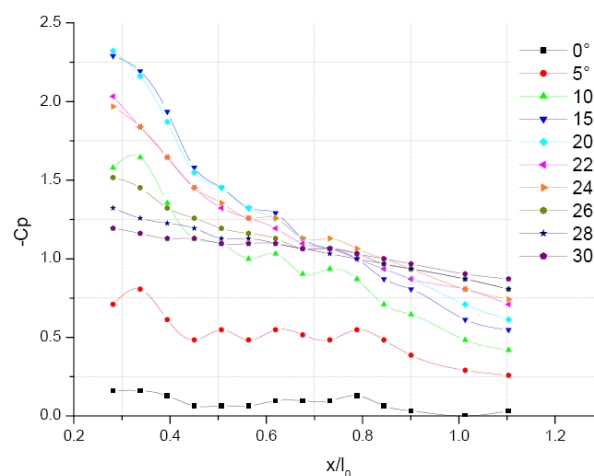**Fig. 2.** Longitudinal evolution of -Cp under the delta wing apex vortex at Re=1.084×10⁵

3. Results and discussion

3.1. Geometry Meshing

A cube of fluid was chosen equivalent to a test section of the wind tunnel. In the center is placed the delta wing model of size well defined at a desired incidence.

The working fluid in the entire is the air with the following properties: ν=1.51 10^{-5}m^2/s and ρ=1.22 kg/m^3.

The studied domain was meshed using Gambit interface. The triangular uniform grid elements were used, with refinement near the surface of the wing where are high fields gradients. To ensure accurate prediction, a fine step of 0.001m was considered. The second order upwind discretization scheme was used for the momentum and modified turbulent viscosity of second order was used for pressure and pressure-velocity coupling using SIMPLE algorithm.

Figure 3 shows the meshed geometry. The flow field around the delta wing contains 3375 cells of grid, with 96 cells along the wing chord and 144 cells along the wing span.
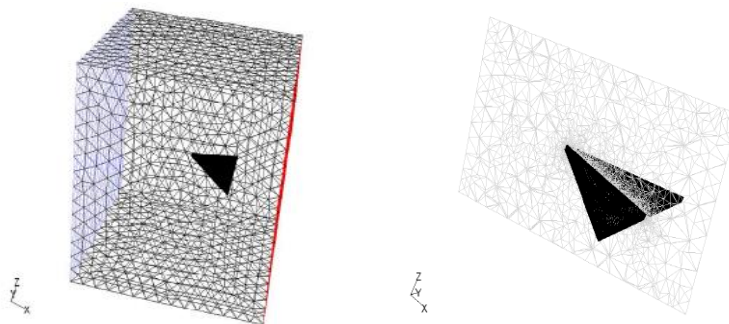

Fig. 3. Meshed geometry. Left: the whole computational space around the wing, and right: the triangular grid of wing faces

3.2. Boundary Conditions

The boundary conditions used here are:

- Velocity inlet at the fluid cube inlet: the free flow velocity was given as 20.3 m/s.
- Outflow on left opposite face: an exit condition without kinetic energy loss.
- Rigid wall on the four other faces of the fluid cube: a condition of adherence without slip. It is also noted that the interfaces (wing-air) are considered as wall boundary.

The effects of turbulence in this simulation were calculated using the one equation Spalart Allmaras model.

3.3. Experimental Validation

Figure 4 shows the longitudinal evolution of the defect pressure coefficient -Cp under the principal apex vortex for *i*=15° and Re=1.084×10^5 along the dimensionless polar coordinate (r/l_0). Three mesh resolutions are used to test the results grid independency. Tested resolutions take 129198, 289429 and 1044683 cells. The results of the two last mesh grids show a convergence along the majority of the polar coordinate extent (r/l_0>0.4) where satisfactory agreement is obtained with measurements. In the following, the grid resolution of 289429 elements will be adopted will be adopted. Besides, the comparison between predictions and measurements shows

that under the principal apex vortex, the peak of aspiration decreases quite similarly (same slope) except near the delta wing apex. The difference between experimental values and numerical results in the range 0.2< r/l_0 <0.4 may be explained by impossibility to control significant turbulence and physically locate the vortex core where higher defect pressure holds. The high turbulence level obtained at the wing apex zone, explain the difference between the experimental and numerical values at the vicinity of the delta wing apex.
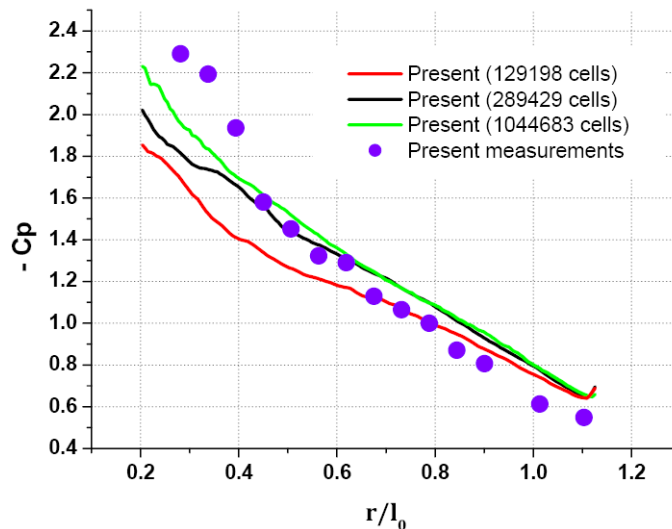

Fig. 4. Longitudinal evolution of -Cp under the principal apex vortex for *i*=15° and Re=1.084×10⁵

3.4. Numerical Results

Figure 5 shows the -Cp contours obtained on the upper and lower faces of the delta wing. The contours reflect the pressure distribution behavior revealing clear indication on the turbulence occurring on the wing faces. It is noteworthy that the two swirls developed on the delta wing suction face are reproduced numerically: The later are represented by two symmetrical zones with significant defect pressure. The aspiration peak of the primary vortex is apparent (red color), the vortex may be identified in the results as an aspiration taking location close to the leading edges. Good agreement with the literature results is also obtained when considering the smoke visualizations of Benkir [20] which indicate that we reproduce the same values of the angle between principal apex vortices α_1 for the case of a thin delta wing, with apex angle β= 80° .

Figure 6 presents curves of maximal defect pressure coefficient -Cp under the apex vortex. This result is in agreement with the experiment. In particular this same Figure 6 shows predominance of the curve corresponding to position x/l_0=0.25 as very close to the delta wing apex. For other sections x/l_0, there is the same trend however the defect pressure coefficient -Cp values become less significant by moving to the wing trailing edge.
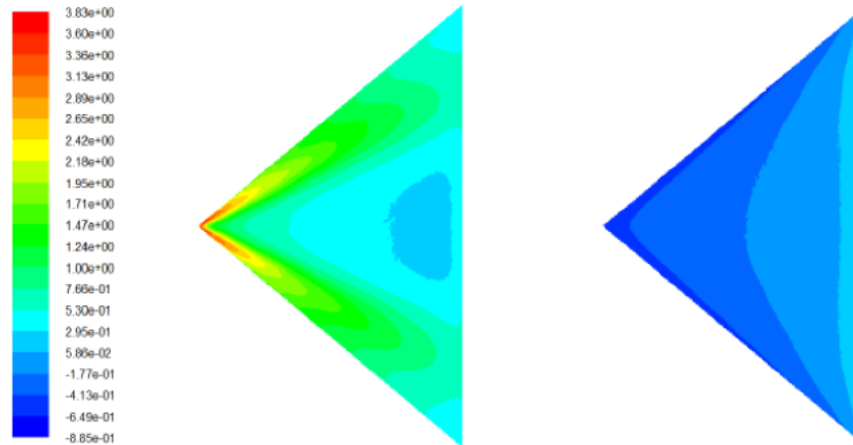
Fig. 5. Contours of -Cp on the delta wing faces at *i*= 15° and Re= 1.084×10⁵.
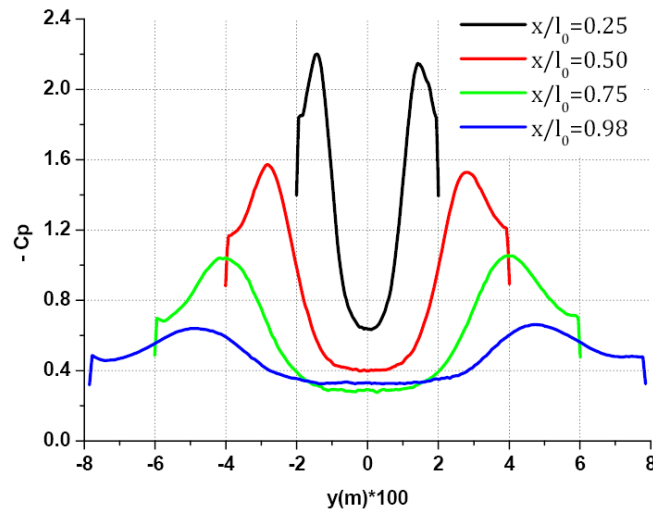Left: on the delta wing upper face (extrados), right: on the delta wing lower
face (intrados)

Fig. 6. Transversal evolution of defect pressure coefficient
-Cp at different cross-sections on the delta wing for *i*= 15°
and Re=1.084×10⁵

Figures 7 and 8 illustrate the external pressure distribution and the values of turbulent modified viscosity, respectively, at two cross-sections according to positions x/l_0=0.25 and 0.75 on the upper and lower faces of the studied delta wing model.
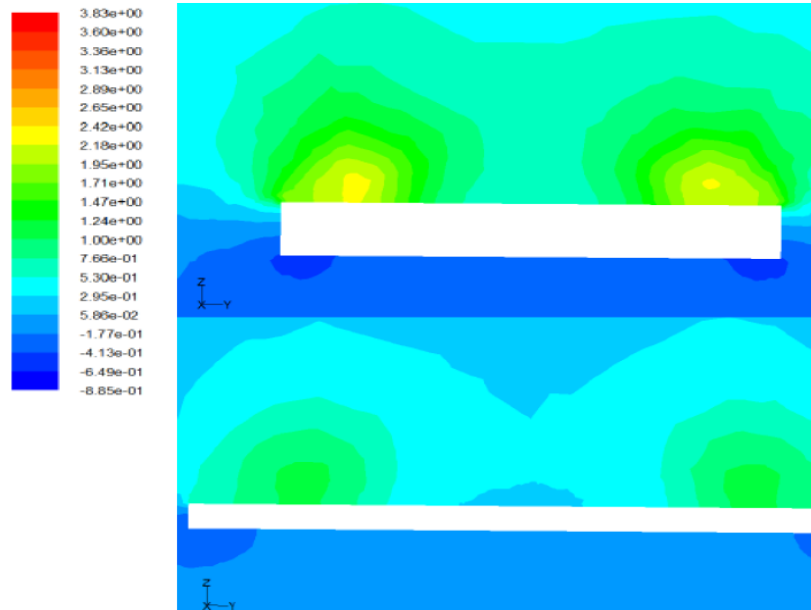
Fig. 7. Defect pressure coefficient −Cp distributions at different transverse sections. Upper: right plan located at x/l_0 = 0.25 and Lower: right plan located at x/l_0 = 0.75
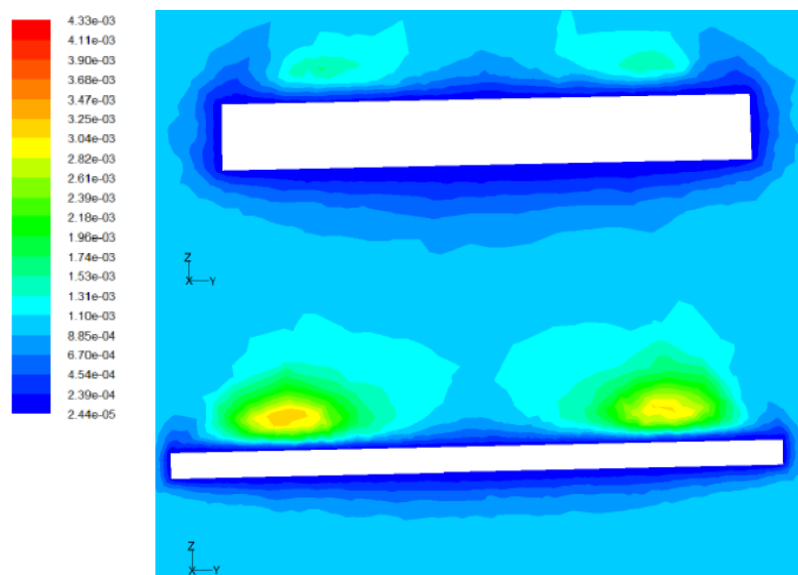

Fig. 8. Modified turbulent viscosity (m²/s) at transverse sections. Upper: right plan located at x/l_0 = 0.25 and Lower: right plan located at x/l_0 = 0.75

The structure is composed mainly by two primary vortices identified on the wing suction upper face. The figures confirm that the area of maximum aspiration peak is maximal at the wing apex and decreases until the position x/l_0 = 0.98 located near the wing trailing edge. It is worth to mention that the flow reaches maximum depression at the apex vicinity and decreases while moving toward the wing trailing edge. Compared to experimental results of reference [13], the levels of defect pressure and the models are in good agreement.

In the present study, different contours are considered according to cross sections x/l_0=0.25, 0.50, 0.75 and 0.98. The sections are selected to show the position of the apex vortices and their intensities while moving away from the wing apex toward the wing trailing edge, the agreement

with the reference experiments [15] seems obvious. Moreover, the assumption of the apex vortices presence appeared with visualizations is increasingly proven. The instantaneous apex vortex location was shown by the maximum depression obtained for each selected cross section.

Figure 9 shows two cross sections for velocity vectors distribution, where lower values (in blue) indicate the viscous vortex center and the higher values (in red) indicate the vortex external limits. The plots clearly indicate the characteristics developing in spirals and extending downstream. The plots in these sections show the cores of vortex through the velocity vectors values. The general tendency is similar to the experiment, noting that simulation can gives sizes and direction of compact velocity. The normal and transverse vortex locations, defined by the positions where there is sign of direction inversion of the velocity components, are in conformity with those indicated in the experiment.
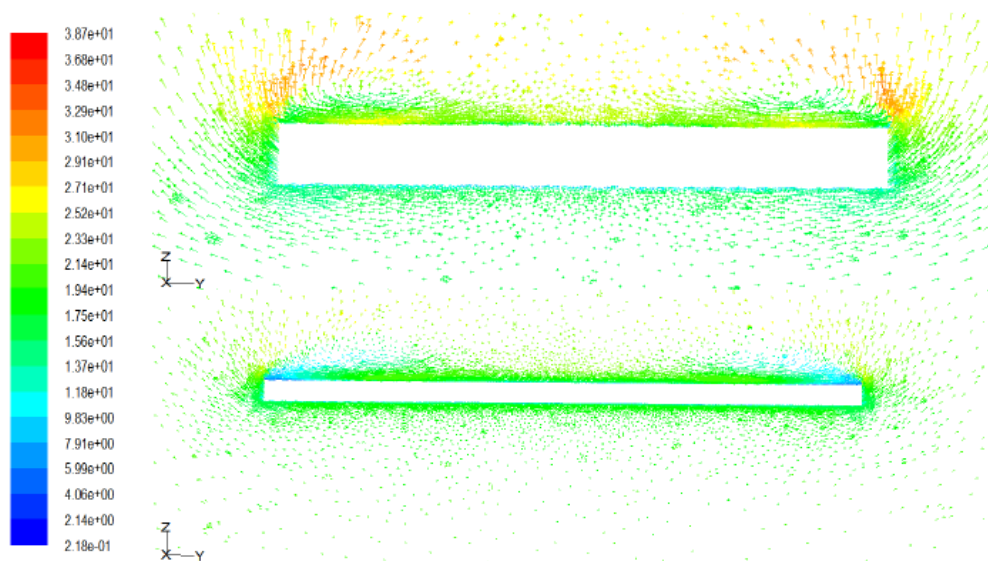

Fig. 9: Velocity vectors evolution at different cross sections on the delta wing. Upper: right plan located at x/l_0 = 0.25 and Lower: right plan located at x/l_0 = 0.75

4. Conclusion

The numerical simulation of turbulent flow at the delta wing suction face, with apex angle β=80° was carried out at incidence angle i = 15° and a flow Reynolds number Re=1.084×10⁵. The characteristics through and along the vortex structure were observed according to the obtained experimental data and are qualitatively well reproduced by simulation. A good agreement between numerical and experimental results was observed for the pressure distribution under the apex vortex developed on the suction face of the delta wing, where the density of grid is relatively refined. The defect pressure coefficient -Cp is maximal near position x/l_0=0.25 as very close to the wing apex. The external pressure distribution and the values of turbulent modified viscosity show that the structure is composed mainly by two primary vortices identified on the wing suction upper face. The flow reaches maximum depression at the apex vicinity and decreases while moving toward the delta wing trailing edge. The plots of the velocity vectors indicate the characteristics developing in spirals and extending downstream.

References

[1] Morton, Scott, James Forsythe, Anthony Mitchell, and David Hajek. "Detached-eddy simulations and reynolds-averaged Navier-Stokes simulations of delta wing vortical flowfields." *Journal of fluids engineering* 124, no. 4 (2002): 924-932.

[2] Kumar, Anand. "On the structure of vortex breakdown on a delta wing." Proceedings of the Royal Society of London. Series A: Mathematical, Physical and Engineering Sciences 454, no. 1968 (1998): 89-110.

[3] Bandyopadhyay, G. "Application of a vortex lattice numerical model in the calculation of inviscid incompressible flow around delta wings." International journal for numerical methods in fluids 10, no. 7 (1990): 729-740.

[4] Hredesh T. and Tide P. S. "Numerical Study on the Effect of Leading Edge Shapes on the Flow Characteristics over Delta Wings". International Journal of Applied Engineering Research 13, no.3 (2018)51-55.

[5] Anwar-ul-Haque, Jawad Khawar, and Sajid Raza Ch. "Influence of turbulence modeling in capturing separated flow over delta wing at subsonic speed." Engineering Applications of Computational Fluid Mechanics 2, no. 3 (2008): 252-263.

[6] Ma, Bao-Feng, Zhijin Wang, and Ismet Gursul. "Symmetry breaking and instabilities of conical vortex pairs over slender delta wings." Journal of Fluid Mechanics 832 (2017): 41-72.

[7] Verhaagen, Nick. "Flow over 50o Delta Wings with Different Leading-Edge Radii." In 49th AIAA Aerospace Sciences Meeting including the New Horizons Forum and Aerospace Exposition, p. 991. 2011.

[8] BRETT, JAMES, and ANDREW OOI. "Effect of Sweep Angle on the Vortical Flow over Delta Wings at an Angle of Attack of 10." Journal of Engineering Science and Technology 9, no. 6 (2014): 768-781.

[9] Nurulhuda Tajuddin, Shabudin Mat, Mazuriah Said, Shumaimi Mansor, "Flow characteristic of blunt- edged delta wing at high angle of attack", Journal of Advanced Research in Fluid Mechanics and Thermal Sciences 39, no.1 (2017): 17-25.

[10] Nadhirah Mohd Zain, Shabudin Mat, Khushairi Amri Kasim, Shuhaimi Mansor, Md. Nizam Dahalan, Norazila Othman, "Wind Tunnel Experiments on a Generic Sharp-Edge Delta Wing UAV Model", Journal of Advanced Research in Fluid Mechanics and Thermal Sciences 40, no. 1(2017): 18-26.

[11] Nelson, R. C., and K. D. Visser. "Breaking down the delta wing vortex." In AGARD Symposium on Vortex Flow Aerodynamics, Netherlands. 1990.

[12] Luckring, James. "Initial Experiments and Analysis of Vortex Flow on Blunt Edge Delta Wings." In 46th AIAA Aerospace Sciences Meeting and Exhibit, p. 378. 2008.

[13] Lok Sun Ko and Tim Lee, "Experimental Investigation of a Slender Delta Wing with Apex and Tail Flap Control", XXIV ICTAM, 21-26 August 2016, Montreal, Canada.

[14] Lee, T., and L. S. Ko. "Aerodynamics and vortex flowfield of a slender delta wing with apex flap and tip flap." Journal of Fluids Engineering 139, no. 5 (2017): 051-106.

[15] Wu, Guangxing. "Experimental Investigation of Asymmetric Vortex Breakdown Flow Control by Microperturbation over Highly Swept Wings." Journal of Aerospace Engineering 31, no. 6 (2018): 04018101.

[16] Zhu, Z. Q., and J. B. Jia. "Numerical simulation of incompressible Navier-Stokes and Euler equations to the vortical flow about a delta wing." Acta mechanica 122, no. 1-4 (1997): 21-31.

[17] Mitchell, Anthony M., and Jean Délery. "Research into vortex breakdown control." Progress in Aerospace Sciences 37, no. 4 (2001): 385-418.

[18] Boumrar, Iddir. "Comportement des Ailes Delta à Apex privilégiés avec et sans Fuselage-Etude Expérimentale et Simulation Numérique." PhD diss., Université Mouloud Mammeri, 2012.

[19] M. Leray, J. P. Deroyon, M. J. Deroyon and C. Minair, « Critère angulaires de stabilité d'un tourbillon hélicoïdal ou d'un couple de tourbillons rectilignes, rôle des angles privilégiés dans l'optimisation des ailes, voiles coques des avions et navires». Association technique et aéronautique, pp. 511-529, session 1985.

[20] Benkir, Mustapha. "Persistance et destruction des structures tourbillonnaires concentrées en particulier au-dessus d'ailes delta: Critères angulaires de stabilité aux écoulements." PhD diss., Valenciennes, 1990.